Electronic Transitions in Biaxially Oriented Polypropylene Accounting for Photo-Stimulated Currents

Duvan Mendoza-Lopez, Laurent Boudou, Laurent Berquez, Christian Laurent, Gilbert Teyssedre

Electronic Transitions in Biaxially Oriented Polypropylene Accounting for Photo-Stimulated Currents

Duvan Mendoza-Lopez[1*], Laurent Boudou[1], Laurent Berquez[1], Christian Laurent[1] and Gilbert Teyssedre[1]

[1]*LAPLACE, Université de Toulouse, CNRS, INPT, UPS,* Toulouse, France

*mendoza@laplace.univ-tlse.fr

***Abstract*— Biaxially oriented polypropylene (BOPP) is a widely used insulating material in capacitor films. As the demand for improved capacitor performance grows, it's crucial to have a deep understanding of polymer molecular structures and their electronic properties. Therefore, focusing on theoretical modeling, simulations, and experiments is important to uncover the relationship between microscopic phenomena and device effectiveness. In this study, we use a recently developed test bench coupling the Laser Intensity Modulated Method (LIMM) and Photo-Stimulated Discharge (PSD) measurements to investigate charge trapping and detrapping processes in BOPP samples. By analyzing photoinduced currents and absorption spectra, we identified relationships between foreign elements within the polymer chains and charge trapping and detrapping dynamics. Our research indicates that BOPP films typically display two light absorption bands in the UV-visible range. The generation of S1 excitons at around 3.1 eV may suggest the creation of free charges through the Auger effect and luminescence emission. Additionally, higher energy photons (~6.2 eV) may contribute to the formation of S2 excitons, influenced by chemical additives such as phenolic antioxidants, which can release electrons under the residual field associated with trapped space charge.**

Keywords*— *Electronic transitions, excitons, polypropylene, photo-stimulated current.

I. Introduction

Biaxially oriented polypropylene (BOPP) is a commonly used insulator in the capacitor film industry, distinguished by its good electrical properties such as low dielectric losses (0.02 %) and large breakdown field (≈ 720 kV/mm) [1]. BOPP films are usually made from highly isotactic polypropylene, characterized by a molecular structure with enhanced regularity giving these films high crystallinity, as well as reduced conductivity and minimized losses [2].

Enhancing the electrical properties of the insulating film in capacitors is crucial for addressing challenges as greater operating temperature and energy density. Enhancements in performance parameters like dielectric constant, dielectric strength, and loss factor undoubtedly benefit the overall capacitor behavior. Achieving these improvements requires the understanding of the molecular scale structure of polymers and their electronic properties. Consequently, researchers are focused on theoretical calculations, simulations, and experiments to elucidate the correlation between microscopic phenomena and device performance.

The experimental investigation presented in this work, complemented by theoretical approaches, employs a new setup that combines LIMM (Laser Intensity Modulated Method) and PSD (Photo-Stimulated Discharge) measurements. This setup enables the study of charge trapping and detrapping processes, along with the exploration of electronic transitions within BOPP samples. This study encompasses discussions on experimental findings, including space charge characterization, PSD recordings, and their interpretation.

II. Materials and Experimental Methodology

A. Samples

The BOPP thin films used for this study were provided by KOPAFILM in Germany and have a thickness of 18 µm. They underwent roughening on both sides to facilitate oil impregnation and enhance film winding during metallization and capacitor production [3]. These BOPP films contain two known additives: penta-erythritoltetrakis (3,5-di-tert-butyl-4 hydroxyhydrocinnamate), known as Irganox 1010, and calcium stearate. Irganox 1010 is used as an antioxidant to stabilize radicals, while calcium stearate acts as both a lubricant and acid trap.

The samples under investigation exhibit transparency and a circular shape, measuring 8 cm in diameter. Gold electrodes, 50 nm thick and 4 cm in diameter, are sputtered on each face of the film, forming the Au/BOPP/Au structure. The bottom electrode consists of a circular layer, also 4 cm in diameter. The top electrode has a specific design, as depicted in Fig. 1, leaving some part of the polymer surface uncovered. Two sample types are examined: one featuring gold electrodes and another with an additional layer of tin-doped indium oxide (ITO), 125 nm thick, in direct contact with the polymer film.

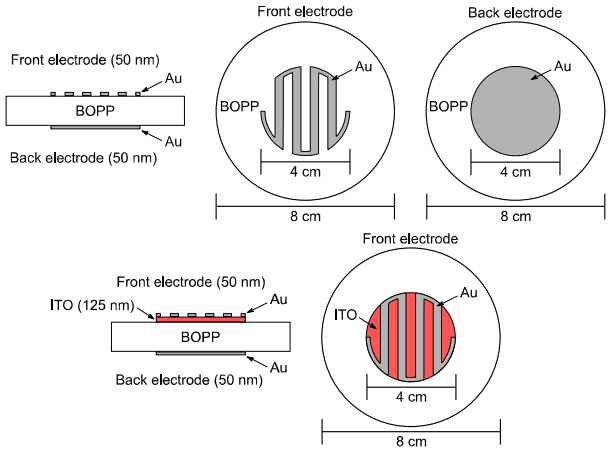

Fig. 1 Schematic representation of the Au/BOPP/Au and the Au/ITO/BOPP/Au sample configurations.

2024 IEEE 5th International Conference on Dielectrics (ICD) | 979-8-3503-0897-6/24/$31.00 ©2024 IEEE | DOI: 10.1109/ICD59037.2024.10613190

This Au/ITO/BOPP/Au structure is employed to establish a distinct conductor-polymer interface from that formed by gold, aiming to extract new data and mitigate edge effects associated with irregular gold electrodes, thus promoting uniformity of the electric field within the insulator. Note that conventional heat treatment at 400°C to enhance electrical conductivity of ITO is impractical for this multilayers sample due to obvious alteration of the polymer's molecular structure.

B. LIMM-PSD coupled setup

The LIMM and PSD methods were integrated into a unified measurement setup [4] to investigate both the formation of space charge and the energetic properties of traps. LIMM is based on the pyroelectric effect, induced by a laser beam heating the front electrode of a metallized sample, to map the space charge profile within the sample. Meanwhile, the PSD technique involves recording photocurrents generated by monochromatic light exposure. The resulting current spectrum reflects charge movement promoted by specific photon energies. These two measurement systems are combined using an automatic switch, facilitating the selection between the two sensing circuits. A sequential measurement protocol is defined in order to analyze the evolution of charge density, detrapping, and electronic transitions. This protocol involves varying external fields from 0 to 200 kV/mm by steps of 40 kV/mm (both in positive and negative polarity voltages), conducting space charge measurements before and after each charging step, and acquiring PSD data after each depolarization period, as outlined in detail in [4].

III. Results

The impact of monochromatic light irradiation on the accumulated charges was investigated by comparing space charge profiles in samples subjected to PSD measurements with those kept in the dark. When samples are polarized with increasing positive voltages applied to the front electrode, the formation of homocharge is observed towards the end of the protocol, i.e. for applied field up to 200 kV/mm extending to a depth of nearly 2 µm, as depicted in Fig. 2 (a). However, space charge profiles exhibit differences when light irradiation is conducted one hour after the end of each polarization interval. The accumulation of positive charge near the front electrode in both Au/BOPP/Au and Au/ITO/BOPP/Au samples is shown to decrease, with lower levels observed in Au/BOPP samples and shallower penetration in ITO/BOPP samples.

When conducting the same experiment with negative voltages, a gradual buildup of negative charges near the front electrode is observed. This accumulation of homocharge near the negative poled electrode becomes notably prominent following the polarization period at -200 kV/mm, with negative charges penetrating to nearly 3 µm from the front electrode. Fig. 2 (b) illustrates that the negative space charge near the negatively poled electrode increases when the sample is pre-irradiated with PSD measurements. Furthermore, negative charges reach a greater depth in Au/ITO/BOPP/Au samples compared to Au/BOPP/Au.

Figure 3 shows the PSD currents recorded for two distinct samples previously charged at 200 kV/mm for one hour and subsequently discharged for one hour. The photocurrent curve for the Au/BOPP/Au sample reveals two peaks. The first peak falls within the energy range of 2.6 eV to 3.4 eV, with the lowest current value occurring at 3.1 eV (398 nm). The second peak, exhibiting a notably higher amplitude, is situated in the energy range from 4.8 eV to 6.5 eV, reaching a current peak at 5.9 eV (208 nm). In contrast, the PSD spectra of the ITO/BOPP sample exhibit a weaker peak between 3.1 eV and 6 eV, with a minimum at 3.9 eV.

When negative voltages are applied to the front electrode, there is a notable change in the amplitude of the PSD spectra, decreasing by a factor of 10, as illustrated in Fig. 4. Photocurrent peaks continue to emerge within the same energy bands, with the peak for the Au/ITO/BOPP/Au sample undergoing the most significant change, shifting to 3.5 eV. It is evident that following periods of negative voltage poling, current peaks exhibit a positive polarity, and conversely in the reverse scenario, aligning with the polarity of the discharge current, which is opposite to that of the charging period.

The light irradiating the samples in this study can directly interact with the polymer, either through areas not covered by the electrode or with the conductive layer. Consequently, the PSD current spectra may arise from phenomena occurring in these two regions. The direct absorption of photons by BOPP stems from the presence of chromophore components in its

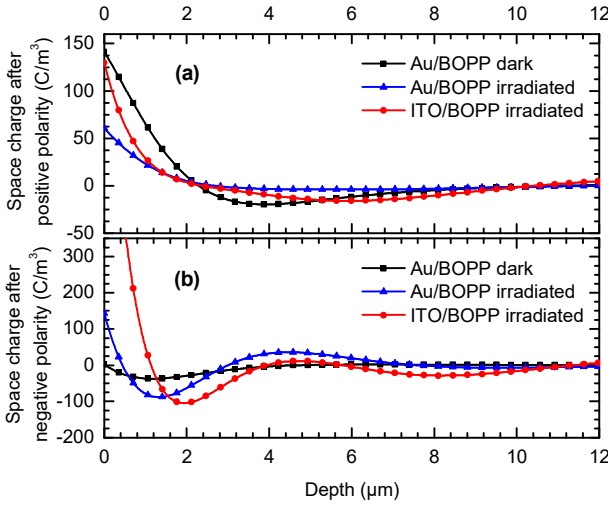

Fig. 2 Space charge profiles of different samples after positive (a) and negative (b) polarity applied fields (+/-200 kV/mm).

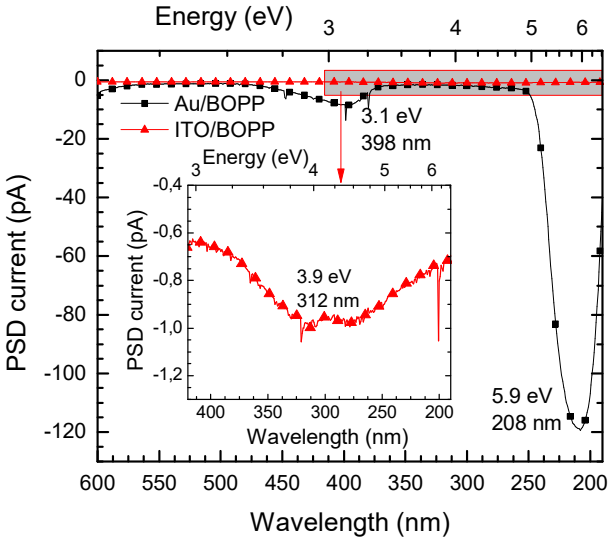

Fig. 3 PSD spectra for different samples after positive poling at 200 kV/mm.

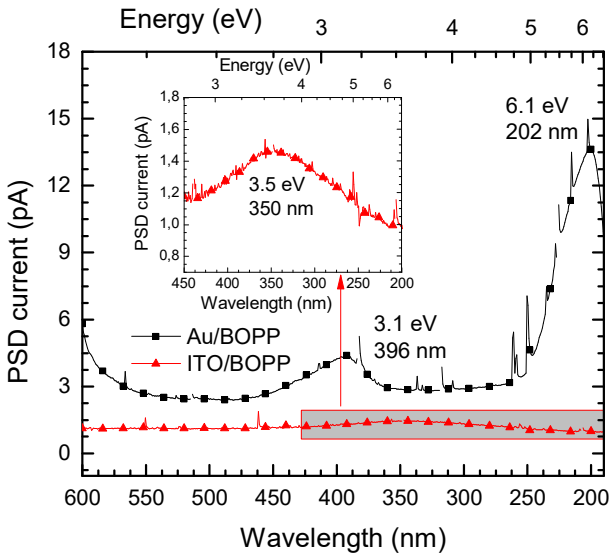

Fig. 4 PSD spectra for different samples after negative poling at -200 kV/mm.

molecular structure. Ho et al.'s work has emphasized the presence of antioxidants, such as Irganox 1010 in BOPP, which exhibit a predominant absorption capacity in the UV range. This absorption induces the formation of chemical derivatives typically displaying absorption peaks around 3.7 eV and 4.9 eV [5].

The peaks observed at 3.1 eV, 3.5 eV, and 3.9 eV do not directly correspond to the absorption bands identified in UV-vis spectroscopy measurements [6]. However, alternative techniques, such as derivative spectroscopy, have revealed bands at 3.12 eV and 3.54 eV, potentially linked to electronic transitions involving transition metal ions like Fe^{3+} [7]. This electronic transition is denoted as S1. The most prominent peak, situated at 5.9 eV, might be associated with a broader absorption band termed S2, encompassing the (π-π^*) transitions of isolated or unsaturated carbonyl groups [7], isolated diene double bonds [8], and/or sterically hindered phenolic antioxidants [5]. Notably, the presence of Irganox 1010 in the BOPP film has been shown to contribute to a band gap at 5.4 eV, as evidenced by reflection electron energy loss spectra [9].

IV. Discussion

Both the Au/BOPP/Au and Au/ITO/BOPP/Au configurations serve as blocking contacts, restricting current injection, given that the theoretical work functions of Au (5.3 eV [10]) and ITO (4.3 eV [11]) exceed the theoretical work function of the polymer, estimated at 2.6 eV [12]. Fig. 5 (a) depicts an energy diagram of the conductor-insulator contact following positive polarization and exposure to light irradiation. During this charging phase, the presence of positive space charge induces an upward bending of the energy bands due to the electric field established between the insulator and the electrode. Upon UV irradiation, the polymer absorbs incident photons, generating excitons near its surface. These electron-hole pairs can dissociate into free charge carriers and attempt to diffuse through the polymer. Positive carriers may traverse the highest occupied molecular orbital (HOMO) level of the polymer and be collected by the metal electrode, facilitated by the internal electric field. Electrons generated by exciton dissociation may become trapped or

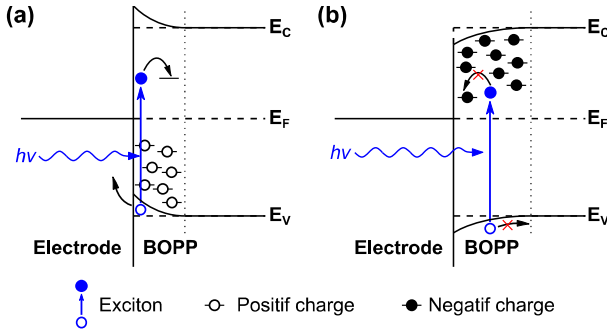

Fig. 5 Schematic diagrams of the metal-insulator contact when irradiated with light. Positive poling (a); negative poling (b).

undergo recombination, thereby accounting for the reduction in positive space charge observed in Fig. 2 (a).

In scenarios where a negative space charge is formed, the charges cause a downward bending of the energy bands, leading to the establishment of an accumulation zone, as depicted in Fig. 5 (b). The excitons generated under these conditions are theoretically less inclined to dissociate or contribute to current flow since conduction sites are unavailable, both within the material volume and at the interface. This circumstance can explain the observed increase in negative space charge illustrated in Fig. 2 (b).

Regarding the origin of PSD peaks, it appears that the peaks at 3.1 eV, 3.5 eV, and 3.9 eV cannot be directly attributed to carrier photoemission from the irradiated electrode. Thus the electron injection barriers, determined by the polymer characteristics and equivalent to 4.8 eV (representing the energy difference between the Fermi level and the lowest unoccupied molecular orbital (LUMO) level of polypropylene calculated using the Density Functional Theory [12], [13]), exceed the energy of these peaks. In this context, the height of the barrier is only consistent with the cutoff energy at 4.9 eV associated with the peak at 5.9 eV, although the maximum value of the highest-energy peak does not precisely coincide with the height of the barrier.

The peaks associated with the S1 exciton could originate from at least two distinct mechanisms. The first hypothesis suggests the release of an electron via the Auger effect. In this scenario, the formation of an exciton from the S0 level with an energy ranging between 3.1 eV and 3.3 eV would generate a hole. Once filled, this hole could induce sufficient energy to trigger the release of a charge. The second possibility involves radiative relaxation of the excited charge [14]. Both of these processes can be amplified by the significant photon flux density emitted by the light source, which falls in the energy band from 2.5 eV to 3.2 eV [4]. Specifically, the cutoff energy of the peak at 3.1 eV aligns with the global maximum of flux density, situated at 2.6 eV, while the current peak corresponds to a local maximum of flux at 3.1 eV. A high photon flux, coupled with a region of low light absorption, may help elucidate the relatively low current peak.

The current peak observed at 5.9 eV after positive poling and at 6.1 eV after negative poling corresponds to the most prominent absorption band in the BOPP film. Consequently, this photo-induced current can be linked to entities that absorb within the energy range between 5 eV and 6.5 eV. These entities may include additives such as antioxidants, carbonyl defects, or diene formations. On one hand, it has been

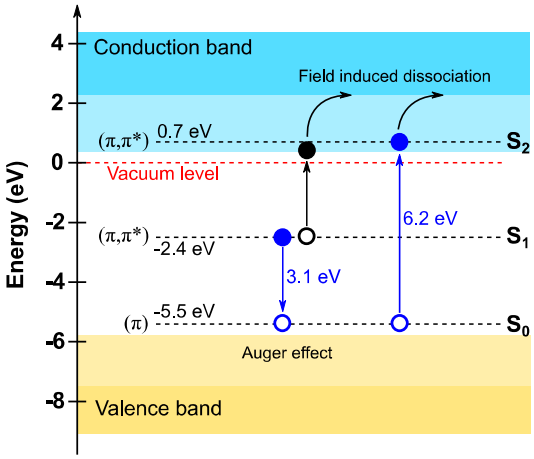

Fig. 6 Schematic representation of the possible electronic transitions within the BOPP film related with the generation of free charges under PSD irradiation.

demonstrated that most chemical defects, such as C=C double bonds, carbonyl groups, and dienes, possess well-defined electronic structures with band transition energies above 5.5 eV [15]. On the other hand, the antioxidant Irganox 1010, with a band gap of 5.4 eV, appears to be a source of deep trapping sites, as observed in various phenolic antioxidants [16], [17]. Once the S2 excitons are generated, they can be dissociated by the local electric field due to their weak binding.

Considering the PSD current peaks observed at 3.1 eV and 5.9 eV in the studied films, along with supplementary insights regarding the Auger effect of the S1 exciton and the electronic transition associated with the S2 exciton of Irganox 1010, we propose the energy scheme depicted in Fig. 6. This diagram provides insights into understanding the intricate processes involved in the generation of free charges associated with PSD photo-discharge currents in BOPP.

V. Conclusion

Space charge formation, trapping/detrapping phenomena and electronic properties were investigated on BOPP thin samples by means of a coupled LIMM-PSD measuring system. The study of light-induced currents, when paired with absorption spectra results, helps identify different external components within the polymer chains. These components impact the processes of charge trapping and detrapping. The BOPP films. under study predominantly exhibit two light excitation bands in the UV-visible range. S1 excitons, generated with energies around 3.1 eV, are potentially linked to transition metal ions, which may release free charges either through the Auger effect or by emitting undissipated energy via luminescence. Photons of higher energy, approximately 6.2 eV, primarily contribute to the creation of S2 excitons, the formation of which is closely associated with chemical additives such as phenolic antioxidants. These high-energy transitions can readily liberate electrons under the influence of the residual field associated with the trapped space charge.

Acknowledgment

The authors, specially DML, acknowledge the support from IEEE DEIS and its graduate fellowship program.

References

[1] T. D. Huan, S. Boggs, G. Teyssedre, C. Laurent, M. Cakmak, S. Kumar, and R. Ramprasad, “Advanced polymeric dielectrics for high energy density applications,” Progress in Materials Science, vol. 83, pp. 236–269, Oct. 2016.

[2] M. Ritamäki, I. Rytöluoto, and K. Lahti, “Performance metrics for a modern BOPP capacitor film,” IEEE Transactions on Dielectrics and Electrical Insulation, vol. 26, no. 4, pp. 1229–1237, Aug. 2019.

[3] I. Rytöluoto, A. Gitsas, S. Pasanen, and K. Lahti, “Effect of film structure and morphology on the dielectric breakdown characteristics of cast and biaxially oriented polypropylene films,” European Polymer Journal, vol. 95, pp. 606–624, Oct. 2017.

[4] D. Mendoza-Lopez, L. Berquez, L. Boudou, and G. Teyssedre, “Measurement setup to simultaneously explore the location and energy of trapped charges in thin polymer films,” Review of Scientific Instruments, vol. 94, no. 8, p. 084705, Aug. 2023.

[5] J. Ho, R. Ramprasad, and S. Boggs, “Effect of Alteration of Antioxidant by UV Treatment on the Dielectric Strength of BOPP Capacitor Film,” IEEE Transactions on Dielectrics and Electrical Insulation, vol. 14, no. 5, pp. 1295–1301, Oct. 2007.

[6] D. Mendoza-Lopez, G. Teyssedre, L. Berquez, and L. Boudou, “Study of Trapping Process in BOPP by Coupled Space Charge and Photo-stimulated Discharge Techniques,” in 2022 IEEE 4th International Conference on Dielectrics (ICD), 2022, pp. 376–379.

[7] N. S. Allen, “A study of the light absorption properties of polymer films using UV-visible derivative spectroscopy,” Polymer Photochemistry, vol. 1, no. 1, pp. 43–55, Jan. 1981.

[8] F. Ş. Boydağ, Sh. V. Mamedov, V. A. Alekperov, and Y. Lenger Özcanli, “Optical characterization of weakly absorbing PP, PE, and PP/PE films,” Opt. Spectrosc., vol. 95, no. 2, pp. 225–229, Aug. 2003.

[9] O. Yuryevna Ridzel, H. Kalbe, V. Astašauskas, P. Kuksa, A. Bellissimo, and W. S. M. Werner, “Optical constants of organic insulators in the UV range extracted from reflection electron energy loss spectra,” Surface and Interface Analysis, vol. 54, no. 5, pp. 487–500, 2022.

[10] Y. Wang, S. Nasreen, D. Kamal, Z. Li, C. Wu, J. Huo, L. Chen, R. Ramprasad, and Y. Cao, “Tuning Surface States of Metal/Polymer Contacts Toward Highly Insulating Polymer-Based Dielectrics,” ACS Appl. Mater. Interfaces, vol. 13, no. 38, pp. 46142–46150, Sep. 2021.

[11] K. Sugiyama, H. Ishii, Y. Ouchi, and K. Seki, “Dependence of indium–tin–oxide work function on surface cleaning method as studied by ultraviolet and x-ray photoemission spectroscopies,” Journal of Applied Physics, vol. 87, no. 1, pp. 295–298, Jan. 2000.

[12] R. Xu, J. Xing, B. Du, M. Xiao, and J. Li, “Improved Breakdown Strength of Polypropylene Film by Polycyclic Compounds Addition for Power Capacitors,” Materials, vol. 14, no. 5, p. 1185, Jan. 2021.

[13] D. Katase, H. Suzuki, M. Kobayashi, A. Kumada, and M. Sato, “Charge Injection Barriers at the Au/Polypropylene and Au/Polyimide Interfaces: The Effect of Polymer Polarity,” in 2023 IEEE Conference on Electrical Insulation and Dielectric Phenomena (CEIDP), 2023, pp. 1–4.

[14] G. Teyssedre, D. Mendoza-Lopez, C. Laurent, L. Boudou, L. Berquez, and F. Zheng, “Charge Trap Spectroscopies in Polymer Dielectrics: Application to BOPP,” presented at the 3rd International Conference on High Voltage Engineering and Power Systems (ICHVEPS), Bandung, Indonesia, 2021.

[15] H.-V. Nguyen and T. H. Pham, “Structural and Electronic Properties of Defect-Free and Defect-Containing Polypropylene: A Computational Study by van der Waals Density-Functional Method,” physica status solidi (b), vol. 255, no. 3, p. 1700036, 2018.

[16] H. Uehara, T. Okamoto, Y. Sekii, S. Iwata, and T. Takada, “Analysis of Charge Trap Depth Using Q(t) Method and Quantum Chemical Calculation in XLPE and PE with Phenolic Antioxidant,” in 2021 IEEE Conference on Electrical Insulation and Dielectric Phenomena (CEIDP), 2021, pp. 454–457.

[17] S. V. Suraci, D. Mariani, and D. Fabiani, “Impact of Antioxidants on DC and AC Electrical Properties of XLPE-Based Insulation Systems,” IEEE Access, vol. 11, pp. 76132–76141, 2023.